Particle-based numerical modelling of liquid marbles: recent advances and future perspectives

C.M. Rathnayaka [1, 2*,] C.S. From [3], N.M. Geekiyanage [2], Y.T. Gu [2], N.-T. Nguyen [4] and E. Sauret [2ǂ]

[1] University of the Sunshine Coast (USC), School of Science, Technology and Engineering, Petrie, Queensland, 4502, Australia

[2] Queensland University of Technology (QUT), Faculty of Engineering, School of Mechanical, Medical and Process Engineering, Brisbane, Queensland, 4000, Australia

[3]Department of Chemical Engineering and Analytical Science, University of Manchester, Manchester M1 3AL, UK

[4] Griffith University, Queensland Micro- and Nanotechnology Centre, Brisbane, Queensland, 4111, Australia.

[*] Email: crathnayaka@usc.edu.au

[ǂ] Email: emilie.sauret@qut.edu.au

Abstract

A liquid marble is a liquid droplet coated usually with hydrophobic particles that can hold a very small liquid volume without wetting the adjacent surface. This combination gives rise to a set of unique properties such as resistance to contamination, low-friction mobility and flexible manipulation, making them appealing for a myriad of engineering applications including miniature reactors, gas sensing and drug delivery. Despite numerous experimental studies, numerical modelling investigations of liquid marbles are currently underrepresented in the literature, although such investigations can lead to a better understanding of their overall behaviour while overcoming the use of cost- and time-intensive experimental-only procedures. This paper therefore evaluates the capabilities of three well-established and widely-used particle-based numerical frameworks, namely Smoothed Particle Hydrodynamics (SPH)-based approaches, Coarse-Grained (CG)-based approaches and Lattice Boltzmann Method (LBM)-based approaches, to investigate liquid-marble properties and their key applications. Through a comprehensive review of recent advancements, it reveals that these numerical approaches demonstrate promising capabilities of simulating complex multiphysical phenomena involved with liquid-marble systems such as their floatation, coalescence and surface-tension-surface-area relationship. The paper further elaborates on the perspective that benefiting from particle-based numerical and computational techniques, liquid marbles can become an even more effective and exciting platform for many cutting-edge large-scale engineering applications.

1. Introduction

Liquid marbles are liquid droplets coated with micro/nanoparticles that are usually hydrophobic, although certain types of hydrophilic particles, such as graphite and carbon black, can also be used for this purpose (Fig. 1) [1-4]. They demonstrate unique characteristics such as soft flexible-and-elastic properties (i.e., micro elastofluidics [5]), ability to contain small liquid volumes without wetting surfaces, resistance to contamination and low friction. Since the initial work reported by Aussillous and Quéré [6], the research on liquid marbles have been mostly based on experimental approaches. The rapid development of micro total analysis systems (μTAS) or 'Lab on a Chip' (LOC) makes the handling of micro volumes of fluids through digital microfluidic technologies critical for the development of fast processes with small amounts of reagent and low contamination [7]. These technologies use droplets to transport and mix small volumes of fluids as required. However, due to the unique properties of liquid marbles associated with digital micro elastofluidics [5], liquid-marble-based microfluidics has become an attractive alternative to conventional droplet-based digital microfluidics [7]. As such, the interest in liquid marbles in μTAS has been growing exponentially with innovative applications being demonstrated [4, 8-11].

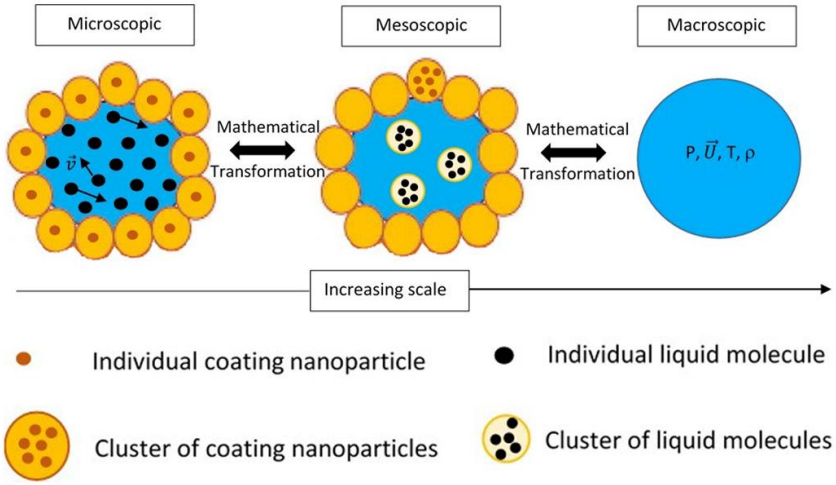

Fig. 1 Components of a liquid marble and the various spatial scales involved.

Magnetic liquid marbles, for example, have demonstrated their potential in biomedical applications and drug delivery [9] as an alternative to conventional discrete microfluidic systems. These magnetic liquid marbles are formed by rolling water droplets on a superhydrophobic magnetic powder such as iron oxide (Fe_3O_4) which forms the marble shell. Magnetic liquid marbles have proven to be highly responsive to external magnetic fields while being able to be opened and closed reversibly using external magnetic forces [12]. This feature

has made them an attractive option for carrying precise amounts of sample through confined and convoluted spaces with respect to biological, chemical and physical applications.

Other applications of liquid marbles include gas sensing [11], carbon dioxide (CO_2) capturing [13], pH sensing [8] and pollution detection [14]. In gas sensing applications, the permeable nature of the liquid marble shell allows the external gas to come in contact and react with the liquid, which in turn changes its colour corresponding to the gas concentration. For pH sensing, the variation of pH affects the integrity and stability of the marble shell, leading to sudden disintegration of the marble at low pH values. Light and heat have also been used to break the shell and release marble content, making such manipulation systems potentially suitable for drug delivery applications. However, these manipulation mechanisms through pH, gases, radiation and magnetic forces have so far been investigated purely experimentally.

Furthermore, liquid marbles have been used as miniature reactors and micro-bioreactors [10], with great potential to grow cells and create controlled micro-environments. The concept is also known as 'lab in a marble' [15]. Further to this hypothesis, composite liquid marbles consisting of two immiscible concentric liquids [16] and water droplets stabilised by another liquid-particle outer layer [17, 18] have recently been reported. With such applications reported in the literature so far, experiments have focused mainly on understanding the material properties and marble behaviour under different circumstances. For example, effective surface tension of liquid marbles has been determined from experimental data [9, 19]. In these experiments, the effective surface tension has been found to be lower than that of pure water, mainly due to the presence of solid particles at the liquid-air interface [12]. One of the challenges faced in the experimental context is the difficulty in determining the relationship between surface area and effective surface tension accurately [20]. The shapes of liquid marbles have also been investigated experimentally. Marbles with radii less than the capillary length exhibits quasi-spherical shapes as the gravitational force is negligible compared to the surface tension force [9]. Here, the capillary length (k^{-1}) is defined as,

$$k^{-1} = \sqrt{\frac{\sigma}{\rho g}} \tag{1}$$

where σ is the effective surface tension of the liquid marble, ρ the density of the liquid and g the gravitational acceleration. As the volume of liquid marble increases, the gravitational force becomes gradually more dominant and it exhibits a puddle shape [21, 22].

The dynamics of liquid marbles can be characterised through dimensionless parameters such as Reynolds number $Re = \rho U D_h/\mu$, Capillary number $Ca = \mu U/\sigma$ and Weber number $We = \rho U^2 R/\sigma$ (where U is fluid velocity, D_h hydraulic diameter, μ dynamic viscosity and R radius of the undistorted marble). Re denotes the relative ratio of inertial and viscous effects, Ca the relative ratio of viscous and surface tension effects and We the relative ratio of inertial and surface tension effects [23, 24]. Mainly owing to the very low velocities in liquid marble applications, Re tend to have relatively low values, usually on the order of 10^{-2} to 10^{0} [25]. For example, in a dynamic deformational analysis of ferrofluid liquid marbles, Nguyen [24] have reported Re values in the range of $0.05 \leq Re \leq 1.12$. Due to the significantly more influential effects of surface tension compared to viscous and inertial effects, the respective values of Ca and We tend to be relatively very low as well. In the aforementioned dynamic deformational analysis of ferrofluid liquid marbles [24], Ca and We values on the order of 10^{-4} and 10^{-5} have been reported, respectively. These value-ranges of Re, Ca and We can generally be considered as representative for most liquid marble applications.

The rolling motion of liquid marbles on different types of surfaces is different from that of pure water droplets [26]. The relatively less-adhesive nature of the marble shell can be given as a reason for this behaviour. The less-adhesive nature and the ability to exchange air across the porous shell enables liquid marbles to serve as an innovative platform for cell culture [27]. Associated with floatation, which increases internal mixing and reduces cell aggregation [10], it can be seen that such a platform could be easily manipulated based on the versatility and low motion-resistance. Liquid marbles have been compressed to test their mechanical robustness [28]. Size of the nanoparticles in the marble shell and the associated hydrophobic/hydrophilic nature have been reported as contributing factors for their robustness. Most of the aforementioned experimental studies have, so far, focused on material properties of a single liquid marble. A wide range of coating materials has been investigated, such as lycopodium, polytetrafluoroethylene (PTFE or Teflon), polyethylene (PE), graphite and silica. Interested readers may refer to Cengiz and Erbil [22] for a detailed table of effective surface tensions and particle sizes and to Oliveira et al. [27] for details on interfacial characteristics of liquid marbles.

Despite recent progress in this research area, many aspects of liquid marbles remain elusive. For instance, the surface area variation of a liquid marble with effective surface tension is difficult to be measured experimentally although a clearer understanding of this phenomenon would be pivotal towards their optimal manipulation [20]. On the other hand, a significant

knowledge gap exists on the variation of effective surface tension with parameters such as marble shell characteristics, capillary interaction and apparent contact angle [20, 29]. Although a number of experimental studies have been conducted on floating liquid marbles as well as their transport and trapping characteristics [15, 19, 30], there is still room for further insights. In addition, the coalescence and splitting processes of liquid marbles are still not well understood [7]. More insights into these processes would be crucial for applications related to chemical and biological assays [12, 31]. Furthermore, the three-dimensional (3-D) morphological behaviour of liquid marbles (e.g., wrinkling of the marble shell) under different circumstances could be further investigated while correlating to subsequent micromechanics [32]. The robustness and lifetime of liquid marbles have also been identified as critical parameters [3, 6] that could benefit from further investigation.

New knowledge on these frontiers can help better design and implement the corresponding experimental procedures while leading to more effective and efficient real-world engineering applications. As such, it is necessary to develop innovative, rigorous, practical and large-scale approaches to efficiently comprehend and optimally manipulate liquid-marble characteristics [27]. In this context, numerical modelling is one of the effective tools that can be used to improve the existing understanding of liquid marbles, and to overcome the use of cost- and time-intensive experimental-only procedures. Such numerical approaches can contribute to more accurate predictions and deeper analyses of the dynamic behaviour of liquid marbles with greater convenience. This new knowledge is likely to inspire new experiments and lead to new discoveries in this sub-domain of engineering. Various existing numerical and computational approaches have the potential to be applied in modelling liquid-marble applications such as floating, coalescence, morphology and micromechanics as well as corresponding property correlations (e.g., surface area and surface tension). Numerical methods have already been applied in comparable contexts such as transport of red blood cells (RBCs) in capillaries [33] and micromechanics of plant cells [34-36]. It would be a tedious and inefficient task to classify the whole range of available numerical and computational approaches as some of these have already been reviewed in equivalent circumstances. Particle-based numerical methods for RBC modelling is an example [37]. Therefore, this paper investigates the scope of particle-based numerical methods applied to simulate equivalent deformable soft matter while discussing their strengths, limitations and future applications only in the context of liquid-marble modelling. In this background, the focus is on the following key applications of liquid marble systems to be modelled with particle-based numerical and computational methods.

- Floating liquid marbles – transport and trapping
- Modelling effective surface tension of liquid marbles
- Coalescence of liquid marbles
- Morphology of the marble shell
- 3-D numerical modelling of liquid marbles

More specific information on these applications is discussed in the upcoming sections.

This paper is organised as follows. Section 2 discusses recent developments of numerical modelling of liquid marbles and corresponding challenges. Section 3 consists of a detailed discussion on specific particle-based numerical modelling methods that demonstrate significant potential to simulate various characteristics of liquid marbles while highlighting their strengths and limitations under different circumstances. Section 4 evaluates the perspectives of utilising these numerical methods to simulate key applications of liquid marbles, followed by overall concluding remarks of the paper.

2. Current developments in modelling liquid marbles and challenges

2.1. Analytical modelling

Analytical models were originally developed to predict specific morphological characteristics (e.g., height, radius etc.) of liquid marbles on solid substrates [38]. They have been combined with experiments to characterise the morphological properties of liquid marbles [6, 19, 39]. The deformation behaviour of floating liquid marbles has been analytically described by Ooi et al. [19], while Wong et al. [39] have employed an analytical modelling approach to demonstrate that the floating behaviour of liquid marbles strongly depends on the interfacial tension of the marble shell. However, these models assume the interface of the floating liquid marble to be purely liquid while considering only one individual static marble. Furthermore, in analytical models developed by Jin et al. [15, 30] for the trapping of floating liquid marbles, the liquid marble has been approximated as a solid volume while disregarding the core liquid component. Thus, analytical approaches have limited capabilities and cannot be conveniently extended to model multiple liquid marbles and the associated complex multiphase phenomena. The development of numerical approaches for liquid marbles is therefore necessary to comprehensively simulate their true behaviour and advanced applications.

2.2. Existing numerical modelling efforts

To the best of authors' knowledge, despite numerous experimental and analytical models [6, 19, 39], only a small number of numerical modelling investigations have been reported on liquid marbles [32, 40]. Polwaththe-Gallage et al. [40] have reported a preliminary two-dimensional (2-D) model including a coating particle-layer and another layer of particles to represent the core liquid using coarse-grained (CG) modelling concepts (Fig. 2). That study focuses on the static behaviour and morphological changes of liquid marbles with different surface tensions. Furthermore, a magnetic force has been applied to the marble shell to demonstrate its ability to open and close the shell selectively [40] (Fig. 3 **(**a)). This model has also been used to establish stress-strain relationships of liquid marbles under compression [32] (Fig. 3 (b)).

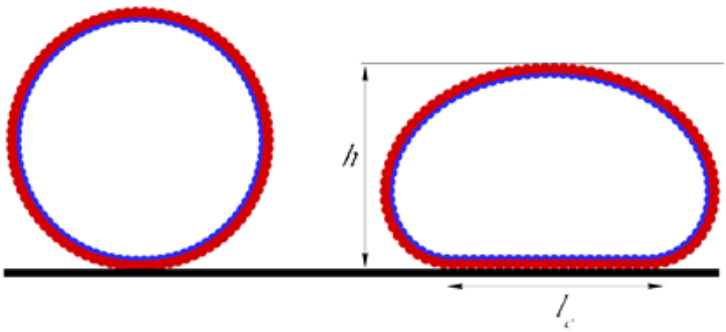

Fig. 2 Results of the existing 2-D CG-based preliminary numerical modelling investigations of liquid marbles where two particle layers represent the coating-particle layer (outer) and the core liquid (inner) [32, 40]

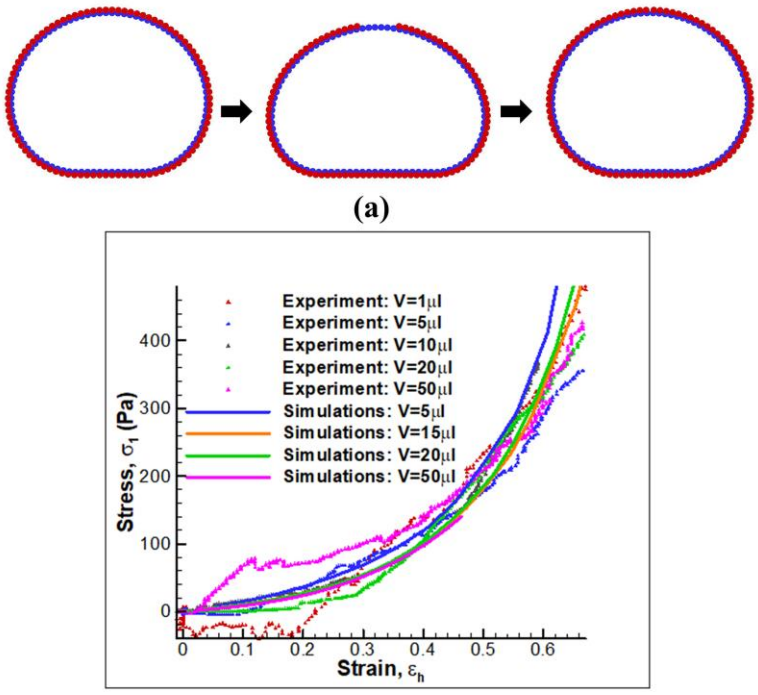

(a)

(b)

Fig. 3 (a) Simulation of opening and closing 2-D liquid marble model under a magnetic force-field [40] and (b) Validation of the compression model for various liquid marble volumes against experimental findings through stress-strain relationships [32]. Reprinted from [40], with the permission of AIP Publishing.

This study has revealed that liquid marbles with smaller Bond numbers take spherical shapes while larger Bond numbers lead to puddle shapes (Fig. 2). The Bond number (Bo) is calculated as,

$$Bo = \frac{\rho g r_0^2}{\sigma} \tag{2}$$

Where r_0 is the equivalent radius of the liquid marble. Moreover, this numerical investigation examined dimensionless height h^* ($= h/r_0$) and dimensionless radius of circular contact area l_c^* ($= l_c/r_0$) of liquid marbles. Subsequent results have shown that,

$$h^* = \begin{cases} 2 & : Bo \ll 1 \\ 2Bo^{-1/2} & : Bo \geq 1 \end{cases} \tag{3}$$

and

$$l_c^* \approx \begin{cases} Bo^{1/2} & : Bo \ll 1 \\ Bo^{1/4} & : Bo \geq 1 \end{cases} \tag{4}$$

which are consistent with the findings from comparable analytical [38] and experimental [24] studies. Although this numerical model has investigated the static behaviour of liquid marbles under various conditions and external forces, it does not consider the dynamic features such as floating, transport, coalescence and splitting. In addition, the approach is limited to 2-D scale while representing the core liquid as a mere quasi-circular particle layer. Thus, this work is yet to be further strengthened with more realistic 3-D modelling and better representation of the internal liquid to begin with. Such an advanced numerical approach can lead to a better understanding of the applicability and efficacy of liquid marbles in practical applications. To the best of authors' knowledge, apart from these studies by Polwaththe-Gallage et al. [32, 40], no further numerical modelling has been reported on liquid marbles yet.

2.3. Challenges in numerical modelling of liquid marbles

One of the major challenges in simulating the realistic behaviour of liquid marbles is the broad range of spatial and temporal scales involved [41]. For example, the length scale may vary from nanometres (nm) for the size of the nano-particles used in the marble shell, to a few micrometres (μm) for the thickness of the overall marble shell, or even up to several hundreds of micrometres and millimetres (mm) for the total characteristic lengths of the marbles. This

broad length scale range is a substantial challenge for numerical and computational methods to be efficiently used in this context [42]. Different numerical approaches may therefore be required to be coupled together to account for the different components of a liquid marble as these components correspond to different spatiotemporal scales (e.g., Fig. 1).

Broadly, numerical methods can be classified based on the spatial scale they solve for (e.g., microscopic, mesoscopic or macroscopic) and the fundamental numerical approach they rely on (i.e., grid-based or particle-based). According to this classification, the most common numerical methods are categorised based on either their discretisation method (grid-based or particle-based) or spatial scale (micro-, meso- and macro-), (Fig. 4). Grid-based methods are commonly used for macroscopic problems and involve methods such as Finite Volumes (FV), Finite Elements (FE) and Finite Differences (FD). These approaches, in general, tend to neglect the effects of individual particles or molecules while assuming a continuum, when solving for the governing equations such as Navier-Stokes equations. This characteristic allows them to be more computationally efficient as they do not model the smallest scales but only cover the largest, both in terms of space and time. These approaches are generally applicable to large industrial-scale applications. The details of the smaller scales, however, can be ignored. Consequently, the validity of the adopted governing equations becomes questionable at smaller scales making them unsuitable at the microscopic scale and beyond.

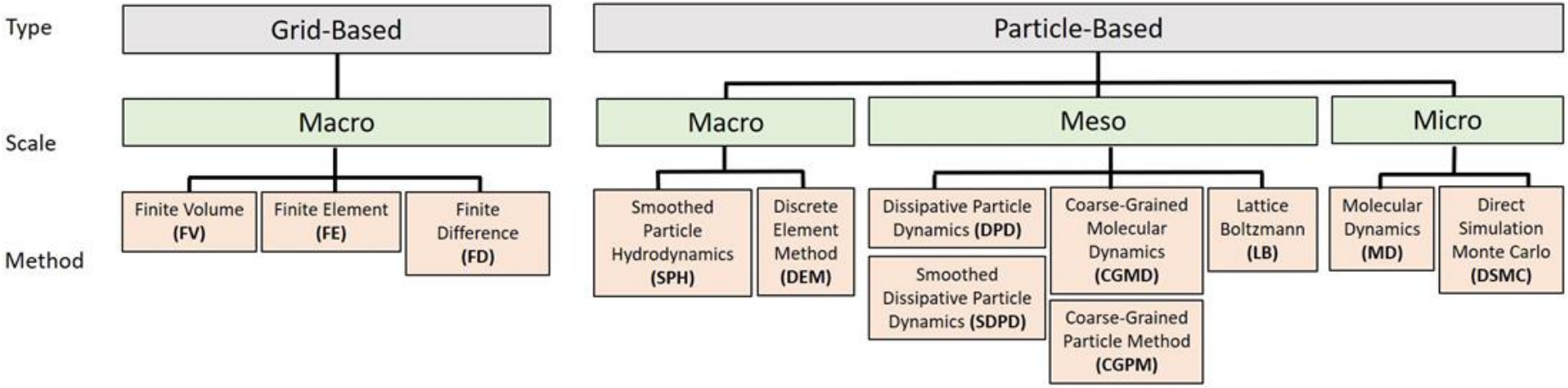

Fig. 4 Classification of existing numerical approaches based on the spatial scales they solve for and the discretisation method they rely on.

Although FE modelling has been used for RBC membranes [43], this approach requires high levels of mesh refinement and can become significantly less efficient for simulating solid-fluid interactions due to the drastically high demands on computational resources [44]. Due to these reasons, grid-based methods would not be further considered in the scope of this paper.

As the scale decreases (i.e., macro to micro), the validity of the governing and constitutive equations used in the macroscopic models becomes questionable due to the continuum assumption. A range of atomistic approaches have been developed to overcome this issue, considering individual interactions of atoms and molecules. Popular atomistic approaches include the Monte Carlo (MC) method and Molecular Dynamics (MD), both of which have proven to accurately account for micro- and nanoscale interactions [45-47]. Despite the high level of accuracy and detailed nature obtained through MD, it has proven to be extremely expensive computationally, taking for example, two years of Graphics Processing Unit (GPU) computations to simulate 1.2 microseconds of 64 million atom trajectories for HIV-1 capsid [48]. Similar issues exist with the Direct Simulation Monte Carlo (DSMC) approaches. As such, both approaches cannot yet be deemed as suitable to model the morphological behaviour or the advanced applications of liquid marbles in a comprehensive manner.

More suitable approaches are found in the domain of particle-based numerical methods, in particular at the macro- and meso- scales. No numerical model has yet been developed to model the 3-D morphological behaviour of liquid marbles nor the corresponding key applications as discussed in the Introduction section. Therefore, an overview of the suitable particle-based numerical modelling approaches is presented in the upcoming section (Section 3) of this paper. These methods have demonstrated significant capabilities in modelling comparable phenomena such as morphological characteristics of deformable soft matter, for instance, RBCs and plant cells. Mechanically, biological cells and liquid marbles can be considered as analogical soft matter due to the presence of an external membrane and internal fluids in their underlying structure. Table 1 lists the comparable components of RBCs, plant cells and liquid marbles in the context of numerical modelling. Accordingly, some modelling techniques that have been widely proven to be suitable for biological cells (e.g., RBCs or plant cells) can be deemed as generally suitable for liquid marbles, subject to relevant modifications. A comprehensive evaluation of such methods is carried out in the upcoming sections of this paper.

Table 1 Comparable components of RBCs, plant cells and liquid marbles in the context of numerical modelling

RBC component	**Plant cell component**	**Liquid marble component**
Internal fluid	Cell fluid	Core liquid
RBC membrane	Cell wall	Marble shell

3. Particle-based numerical modelling techniques for liquid marbles

This section offers an overview of the potential particle-based numerical modelling approaches suitable for studying liquid marbles, their morphological behaviour and corresponding applications. In doing so, specific focus has been placed on the capabilities to numerically represent fundamental aspects such as fluid-fluid interactions, fluid-solid interactions, solid-solid interactions and subsequent dynamics.

3.1. Smoothed Particle Hydrodynamics (SPH)-based approaches

SPH is one of the most widely used meshfree particle methods (MPMs) [49]. In SPH, a given problem domain is represented through a set of particles which are not interconnected through a fixed grid. These particles carry the properties of the corresponding medium and interact with each other inside a range defined by a smoothing kernel function [50, 51]. Each SPH particle represents a small local portion of the problem domain, while moving with the fluid volume [52]. Pressure of the fluid is derived through an equation of state using density. The effect of viscosity could be incorporated into the viscous flows through particle accelerations. Governing conservation equations such as Navier-Stokes equations are numerically discretised on particles and consequently, field properties such as density, velocity and acceleration are computed based on the influence domain of corresponding particles [49, 53]. Conservation of mass is naturally incorporated into SPH as it is a Lagrangian particle method. SPH particle schemes dynamically evolve in space as well as in time. Generally, it can better handle large deformations, multiphase phenomena and multiphysics associated with fluid mechanics compared to the classical grid-based approaches, which is an added advantage for modelling liquid marble phenomena [49, 54]. Further, SPH-based computational approaches have specifically demonstrated promise on modelling low-Re phenomena [54, 55].

Accordingly, the continuity and momentum equations are represented in SPH as,

$$\frac{\mathrm{d}\rho_i}{\mathrm{d}t} = \sum_{j=1}^{N} m_j(\boldsymbol{v}_i - \boldsymbol{v}_j).\nabla_i W_{ij} \tag{5}$$

$$\frac{\mathrm{d}\boldsymbol{v}_i}{\mathrm{d}t} = -\sum_{j=1}^{N} m_j\left(\frac{P_i}{\rho_i^2} + \frac{P_j}{\rho_j^2}\right).\nabla_i W_{ij} + \sum_{j=1}^{N} m_j \frac{m_j(\mu_i + \mu_j)(\boldsymbol{r}_i - \boldsymbol{r}_j).\nabla_i W_{ij}}{\rho_i\rho_j|\boldsymbol{r}_i - \boldsymbol{r}_j|^2}.(\boldsymbol{v}_i - \boldsymbol{v}_j) + \boldsymbol{f} \tag{6}$$

where ρ is the density, μ the dynamic viscosity, $\boldsymbol{v}$ the velocity, P the pressure, $\boldsymbol{f}$ the external force acting on fluid. Also, i represents the particle of interest and j the surrounding particles. N is the total number of particles and m the mass of particles. W_{ij} is the smoothing function value, which is equal to $W\ (\boldsymbol{r}_i - \boldsymbol{r}_j,\ h)$, h being the smoothing length.

Due to its robustness, SPH numerical framework can also be used for multiscale investigations [56] as well as for non-Newtonian fluid modelling [57, 58]. For example, it has shown the ability to be coupled with MD or Dissipative Particle Dynamics (DPD)[59] for multiscale applications especially in biophysics and biochemistry [49]. These capabilities make SPH-based methods an attractive candidate to model liquid marbles. To further demonstrate this phenomenon, numerical modelling studies that have modelled comparable soft matter using SPH-based approaches will be discussed below.

3.1.1. Numerical attempts to model comparable soft matter using SPH

SPH has been used in combination with DEM and CG to model different types of biological soft matter such as plant cells. Van Liedekerke et al. [55, 60, 61] have employed a coupled SPH-DEM approach to numerically model plant cells and tissues. A further developed SPH-DEM approach has been utilised to model 2-D drying and shrinkage characteristics of plant cells by Karunasena et al. [34, 62, 63]. In that work, cell fluid has been modelled with SPH, while Discrete Element Method (DEM) has been used to represent the cell wall. Based on an equivalent numerical framework, 3-D plant cell drying computational models have also been developed using either SPH-CG [64, 65] or SPH-DEM approaches [66]. In these studies, the cell fluid and cell wall have been modelled in a highly comparable manner to the core liquid and shell of a liquid marble, respectively.

Furthermore, there are numerous efforts to numerically model mechanics of RBCs using SPH-based approaches. Coupled with SPH, DEM has been extensively applied to model RBCs [37, 67]. In these work, different sets of SPH particles represent both plasma and RBC, while DEM has been used to model the membrane. For instance, Wu and Feng [68] have used SPH to investigate the transit of healthy and infected RBCs in microchannels. In an equivalent

approach, Polwaththe-Gallage et al. [33, 69] have used a coupled SPH-DEM approach to predict the deformation of RBCs when flowing through narrow 3-D capillaries. RBC membrane has been discretised as a set of DEM particles connected through attractive and repulsive forces, while haemoglobin inside the RBC and the plasma has been modelled using SPH. In doing so, the membrane and the internal fluid of an RBC have been numerically modelled in a comparable manner to the respective components of a liquid marble. Accordingly, there is a strong possibility to use an SPH-DEM or SPH-CG approach to model liquid marbles, their 3-D morphological behaviour and advanced applications due to the similarities existing across comparable components of RBCs, plant cells and liquid marbles as given in Table 1. More details on this aspect is discussed in the Section 4 of this paper.

3.1.2. Limitations of SPH-based approaches

When modelling biological tissues consisting of large numbers of cells, the computational cost of either an SPH-DEM or SPH-CG approach significantly increases due to the fundamental nature of SPH computational framework. For instance, the computational resources required for the neighbour-particle-searching process in SPH calculations increase exponentially when the number of particles in the problem domain increases significantly. This is one of the critical issues when modelling large arrays of liquid marbles. However, GPU-based computing has been recently suggested as a potential technique to overcome this challenge [70-72]. Further, it can be numerically challenging to incorporate thermal fluctuations into an SPH-based computational framework. This is a crucial concern as the nanoparticles in the marble shell may require thermal effects to be determined, particularly for applications where they are guided by external force-fields such as magnetic or electric forces. For example, the activation of liquid marble coalescence or splitting [73]. Table 2 (a) summarises the strengths and limitations of SPH-based approaches in the context of liquid marble modelling.

3.2. Coarse-Grained (CG)-based approaches

Coarse-graining is the computational representation of a larger cluster of particles through a smaller number of particles while capturing the associated physical characteristics as accurately as possible [74-76]. The primary benefit of the CG technique is the significant reduction of computational cost, which will otherwise be impractical when numerically representing each particle of the corresponding cluster. The degree of coarse-graining has direct implications on the level of numerical discretisation and therefore affects the level of details represented, computational efficiency and, more importantly, accuracy. The strength of CG for studies

associated with liquid marbles has already been demonstrated through a couple of recent investigations by Polwaththe-Gallage et al. [32, 40] as previously discussed in Section 2.2. These numerical investigations are based on the 2-D application of CG concepts to predict the morphological behaviour of magnetic liquid marbles and their compression. Even though these studies have proven to be suitable for preliminary investigations of symmetric and homogeneous liquid marbles, in reality, liquid marbles can be asymmetric and heterogeneous. Comprehensive consideration of coating particles in the marble shell and the dynamics of the surrounding media (i.e., solid or fluid) are crucial for biomedical applications such as disease modelling, drug screening, targeted drug delivery, cell culturing and blood typing [4]. Therefore, a comprehensive 3-D numerical representation of liquid marbles would be desirable, and CG is an appropriate candidate as an efficient and accurate computational method to fulfil this requirement.

From a numerical perspective, strong similarities can be observed between modelling liquid marbles and biological cells (e.g., Table 1). For example, a variety of studies has been reported in the literature where CG has been successfully employed to explore the mechanical, rheological and dynamic properties of RBCs under diverse circumstances [74, 75, 77-90]. The notable feature of these studies is the application of CG in different spatial scales. For example, Li and Lykotrafitis [74] have applied the CG technique at the molecular level, which is also known as coarse-grained molecular dynamics (CGMD), to model the RBC membrane by representing clusters of molecules that are located in the lipid bilayer and the cytoskeleton. A couple of the benefits of CGMD are the provision of high-level details and being suitable for investigating heterogeneous characteristics of different molecular structures at a reasonable computational cost. This approach, however, remains computationally expensive to be fully utilised for large-scale simulations of multiple liquid-marbles, unless used in a multiscale framework. In the coarse-grained particle method (CGPM), a meso-scale representation has been achieved through clustering several virtual particles together. This approach has been successfully employed for mesoscopic and macroscopic investigations of RBCs where the heterogeneous nature of the RBC membrane is satisfactorily approximated via its properties for length scales above a certain value [91-93]. For example, Fedosov et al. [94] have developed a CGPM approach to predict membrane mechanics of healthy and diseased RBCs undergoing mechanical deformations.

Numerous investigations that employ CG in RBC research provide evidence that CG technique can be applied for advanced studies on liquid marbles. It can be deduced that CG is appropriate

to model liquid marble shell, where accurate representation of the coating-nanoparticle characteristics is necessary. For example, the systematic coarse-graining of a liquid marble shell can yield a model with a smaller number of representative particles compared to a finer more-detailed version. Therefore, the relationship between the particle spacing of the coarse-grained (l^c) and finer (l^f) liquid marble surfaces can be represented as follows, considering the average increment of surface area per particle [77, 94].

$$l^c = l^f \sqrt{\frac{N^f - 2}{N^c - 2}} \tag{7}$$

where N^f and N^c are the number of representative particles on the finer and coarse-grained liquid marble surface, respectively. This relationship is an indicator of the area representation of each particle for the coarse-grained and finer liquid marble surfaces. Similarly, the remaining model coefficients need to be estimated at the intended level of coarse-graining such that the liquid marble characteristics can be accurately represented. Therefore, CG technique enables accurate and efficient prediction of liquid marble behaviour where surface properties (e.g., surface tension, wettability and deterioration of the marble shell) play a key role. Even though CGPM is a suitable candidate to explore surface phenomena in liquid marbles, CGPM alone is unable to incorporate the liquid phase into the research problem. Accordingly, CGPM needs to be coupled with another numerical method (i.e., SPH, Lattice Boltzmann Method (LBM) or DPD) to represent phenomena in the fluid phase. Consequently, each individual study should carefully consider these effects and establish a critical trade-off to satisfy the objectives of the applications as later discussed in the Section 4 of this paper. Table 2 (b) summarises the strengths and limitations of CG-based approaches in the context of liquid marbles.

3.3. Lattice Boltzmann Method (LBM)-based approaches

LBM, a mesoscale approach based on the kinetic theory of gases, has proven to be an attractive alternative numerical method to solve the Navier-Stokes equations. In LBM, a distribution function, f, is used to describe the fluid flow that takes the following general form,

$$f_\alpha^\phi(\boldsymbol{x} + \boldsymbol{\xi}_\alpha \Delta t, t + \Delta t) = f_\alpha^\phi(\boldsymbol{x}, t) + \Omega_\alpha^\phi(\boldsymbol{x}, t) + \Omega_\alpha^{S,\phi}(\boldsymbol{x}, t) \tag{8}$$

where $f_\alpha^\phi : \alpha = 0, \dots, Q$ is the αth discrete lattice distribution of a lattice structure of size Q of each ϕ fluid species/component in $\boldsymbol{x}$ is space and t is time. The left-hand side term in Eq. 8, $f_\alpha^\phi(\boldsymbol{x} + \boldsymbol{\xi}_\alpha \Delta t, t + \Delta t)$, is the direct and exact advection of particles, commonly referred to as

the streaming step. This is one of the unique qualities of the LBM approach that ensures *zero* 'numerical'-diffusion, a clear advantage compared to fractional advection in finite solvers. The first collision operator, Ω_{α}^{ϕ}, allows for hydrodynamics to be simulated, and its most basic form is given by single-relaxation-time,

$$\Omega_{\alpha}^{\phi}(\boldsymbol{x},t) = -\frac{\Delta t}{\tau^{\phi}}\left[f_{\alpha}^{\phi}(\boldsymbol{x},t) - f_{\alpha}^{\phi,eq}(\boldsymbol{x},t)\right] \tag{9}$$

where the relaxation τ^{ϕ} based on kinematic viscosity of the fluid, i.e., $\nu^{\phi} = c_s\left(\tau^{\phi} - 1/2\right)$, with c_s being the lattice specific sound speed. The second collision operator, $\Omega_{\alpha}^{S,\phi}$, accounts for all relevant source terms to be coupled into the LBM collision operator (Eq. 8), e.g., interaction forces between the various fluid and solid phases, and is the basis of flexibility and adaptability of LBM for modelling complex fluids [95], such as liquid marbles.

Unlike traditional methods, with the LBM mesoscopic approach, the Navier-Stokes equations are not discretised directly. The Lattice Boltzmann equations are instead discretised by a lattice structure set $\{w_{\alpha}, \boldsymbol{\xi}_{\alpha}: \alpha = 0, \ldots, Q\}$, with discrete lattice velocities $\boldsymbol{\xi}_{\alpha}$ and weights w_{α} that can recover the equilibrium distribution function f_{α}^{eq} at certain order of approximation of the Maxwell-Boltzmann equation. LBM has demonstrated its ability to go beyond the validity range of Navier-Stokes equations with higher-order Lattice Boltzmann models, consisting of higher-order expansions in conjunction with higher-order lattice structures [96]. LBM has become a popular approach for modelling microscale fluid dynamics thanks to its accuracy, adaptability [97] and flexibility to model complex flows [37, 95]. LBM computations are inherently parallel with high scalability. The reason behind this is two-fold: (a) the stream-collide process and (b) hydrodynamic variables being obtained by simple summation of the discrete distribution function. As such, LBM can be directly implemented through GPUs [98] opening the opportunity to solve complex, large-scale simulations approaching the exascale (i.e., in the order of 1×10^{18} computing operations per second) [99].

Moreover, multiscale approaches have been developed for modelling fluid flow, specifically using multiscale LBM [100, 101]. For example, LB-MD approach has been proposed to account for nano-scale roughness of microchannel walls [102]. Other multiscale approaches for fluid flow have also been developed to model oil and gas flow interactions with granular rocks from natural reservoirs [103]. While the accuracy of this multiscale LB-MD approach is high, the computational cost is also extremely high, which may limit its practical applicability for modelling arrays of liquid marbles. The success of LBM in a myriad of complex multi-

physics applications is owed to its flexibility in incorporating source terms [95, 99]. The application of LBM for liquid marbles requires multiple physical aspects to be properly facilitated, namely to account for multiphase, multicomponent features and the marble shell (i.e., solid-phase phenomena), which are discussed in detail in the following subsections.

3.3.1. Multiphase/Multicomponent LB methods

LBM has seen significant success in a broad range of applications involving multiphase and multicomponent flows [104, 105] including specific problems related to chemical engineering [106]. In general, there are three LBM methods for simulating multiphase/multicomponent flows, namely the free energy model [107], colour-gradient model [108] and pseudopotential model [109]. Li et al. have presented a complete review of these LBM methods [110], while Krüger et al. have provided an insightful review of the free-energy and pseudopotential models [104].

Recent work has revealed promising results for single-phase and multi-phase binary non-ideal fluid mixtures [111, 112] using high-order LBM pseudopotential models. The advantage of using high-order LBM is that the higher-order lattice structure conforming to higher isotropy gradients in conjunction with higher-order expansions allows for higher-order moments of the distribution to be recovered, which allows for Galilean-invariant LB models. Furthermore, a high-order lattice structure with the pseudopotential method allows for controlled interactions at various Brillouin zones, known as multi-range pseudopotential [113]. This approach, for a high-order lattice structure that covers two Brillouin zones, has been successfully applied to study complex multiphase/multicomponent phenomena, most notably soft flowing crystals and emulsions [114, 115]. Furthermore, the complex droplet dynamics of coalescence on superhydrophobic surfaces have been studied using the pseudopotential [116] and the free-energy models [117]. The use of these multiphase/multicomponent LBM models for studying complex fluid surface phenomena is covered in the following subsection. In summary, LBM for multiphase and multicomponent flows has already seen significant success in a myriad of engineering applications and allows for the investigation of various complex states of matter.

3.3.2. LBM with Fluid-Structure Interaction

LBM allows for various complex fluid-structure phenomena to be studied using multiphase/multicomponent models to account for fluid-structure interactions (FSI) [111, 118], including two-phase slip-flow over structured surfaces [119], geometrically patterned surfaces [120], and chemically patterned surfaces [121, 122]. In addition, the multi-range

pseudopotential approach reported by Falcucci et al. [113] allows for the study of stress-induced cavitation [123]. Furthermore, using the free energy model, Sadullah et al. and Panter et al. have recently been successful in studying the bidirectional droplet motion over surfaces with topographical gradients [124] and design optimization strategies for superomniphobic textured surfaces [125], respectively.

Popular approaches to include FSI in LBM for deformable solids have been extensively covered by Krüger et al. [104], such as the bounce-back (BB) approach (standard BB and interpolated BB) and interpolation schemes. Since LBM is inherently a fluid-solver, simulating the dynamics of solid particles requires LBM to be coupled with another numerical approach to model the marble shell (i.e., dynamics of solid particles). Due to the symmetric square lattice requirement in LBM, interpolation between the lattice (i.e., Eulerian grid) and the solid particles, which reside as Lagrangian points, is required to account for FSI. The Immersed Boundary method (IBM) has been a prevalent and successful approach to achieve this coupling [104]. Hereinafter, LBM coupled with IBM is denoted by LB-IB, for convenience. LB-IB coupling has been used to model interactions of the continuous fluid phase in soft matter such as cells, for example, to model RBC flows, as already covered in the extensive review by Ye et al. [37]. For example, the Palabos Library is an open-source framework based on LB-IB that has been successfully employed to simulate cellular blood flow in 2-D and 3-D [126, 127]. However, 3-D LB-IB implementations for soft matter modelling are clearly lacking in the literature, mainly due to the computational cost associated with this approach.

Compared to LB-IB, coupling LB-IB with DEM (LB-IB-DEM) can allow for the implementation of solid particles (marble shell) with physical properties (e.g., mass, temperature, and conductivity) [128, 129]. Here, the IB forcing terms are needed to track and couple the individual liquid marbles (i.e., DEM particles) to the fluid grid, i.e., FSI. LB-IB-DEM has already been successfully applied mostly in multiphase flows where the carrier fluid has been modelled using LBM while DEM has been used to model solid particles flowing with the carrier fluid [130, 131]. For a liquid marble to be modelled via this approach, the surface tension effect must be incorporated through FSI directly, i.e., the coupling between LB, IB, DEM, and a multiphase/multicomponent model. More specifically, while DEM can allow for the implementation of solid particles and their physical properties, the chemical effects of the marble shell (e.g., a hydrophobic surface) need to be implemented with a different approach. The LB-IB-DEM approach could potentially account for these chemical surfaces by using, for example, the pseudopotential or free energy model, which, as mentioned previously, has

already seen success in modelling chemically patterned surfaces [118, 119]. Such an LB-IB-DEM approach can potentially allow for modelling the rupture and coalescence of the marble shell under contact.

3.3.3. Closing Remarks on LBM for Liquid Marbles

LBM has all the right ingredients for complex flows, e.g., flexibility and efficiency, making it an attractive candidate for numerical modelling of liquid marbles. Ultimately, to simulate a liquid marble with an LBM approach require the addition of multiple numerical methodologies (or, at the very minimum, one additional method) to simulate the rupture and coalescence of the marble shell. Some of the potential avenues to achieve this have been discussed in the previous subsections. It should be noted that LBM can be coupled with virtually any other numerical method/model due to its flexible source term. Though LBM has the advantage of computational efficiency (the inherent locality and parallel scalability), a consequence of including the external methods (for the purpose of simulating liquid marbles) can be the partial-loss of this feature due to either the nature of the computational framework of the external method and/or the coupling between various numerical methodologies. Having said that, developing parallel and efficient methods is possible. Strengths and limitations of using LBM-based approaches to numerically model liquid marbles have been summarised in Table 2 (c). The upcoming Section 4 of this paper discusses the key applications of particle-based numerical modelling in the scope of liquid marbles and provides future perspectives.

4. Perspectives of particle-based numerical modelling for liquid marbles and future applications

4.1. Floating liquid marbles – transport and trapping

Liquid marbles demonstrate the unique ability of stably floating on liquid surfaces and even moving across the free liquid surface with no leakage and low evaporation [30]. The non-wetting behaviour and the lower friction provide floating liquid marbles a significant level of mobility [29] which opens up many interesting possibilities in areas such as drug delivery, gas-sensing and pH-sensing [132]. Numerous factors in a floating liquid marble system can potentially be utilised to control the movement and trapping: e.g., career liquid properties, core liquid properties, coating particle properties, volume of the liquid marble, apparent surface area of the liquid marble and self-propulsion of a liquid marble through Marangoni effect [29] (Fig. 5) .

Table 2 Strengths and limitations of different particle-based numerical methods in the context of liquid marble modelling

Modelling method	**Strengths**	**Limitations**
a) SPH-based approaches (Section 3.1)	• Have already been used to model red-blood cells (RBCs) and plant cells which are numerically comparable soft matter to liquid marbles • Ability to model non-Newtonian fluid flows which could be advantageous for complex fluid-flow-related applications • Can be used for multiscale numerical investigations	• Difficulties in handling thermal fluctuations • Limitations in modelling the dynamic behaviour encountered during coalescence • Exponentially increasing computational cost when the number of particles in the problem domain increases significantly
b) CG-based approaches (Section 3.2)	• CGMD o High level of detail o Reduced computational cost compared to a full Molecular Dynamics (MD) simulation o Ability to model surface tension and wettability characteristics of the marble shell o Ability to model the deterioration of the marble shell and coalescence process o Ability to accurately characterise the interactions between marble shell and core liquid • CGPM o Reduced computational cost compared to CGMD o Ability to model the whole marble	• CGMD o Highly computationally expensive to be used for multiple liquid marbles unless used in a multiscale framework o Only a smaller section of a liquid marble could be modelled due to excessive computational cost • CGPM o Comparatively less amount of details of the problem domain could be modelled compared to CGMD o Needs to be coupled with another numerical method to incorporate liquid phase phenomena (e.g., SPH or LBM)
c) LBM-based approaches (Section 3.3)	• Ability to model complex single-phase binary fluid mixtures • Capacity to be extended from microscale to mesoscale through multiscale techniques • Computational efficiency due to inherent parallel processing abilities • Ability to be directly processed through GPUs • LB-IB-DEM can overcome the LB-IB limitation of not considering the marble shell	• 3-D LB-IB-DEM models tend to be highly computationally expensive • Difficulty in modelling marble shell realistically • LB-IB-DEM has difficulties in accurately modelling thermal variation • Needs to be coupled with another numerical method to incorporate the dynamics of solid particles (i.e., marble shell), e.g., IB, DEM, or the combination of both IB-DEM.

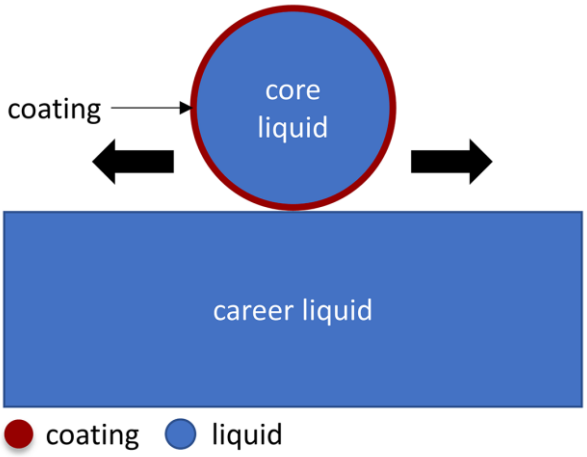

Fig. 5 Components of a floating liquid marble system

The lifetime, robustness and mobility of a floating liquid marble have direct correlations with the surface tension of the career liquid [29]. However, these correlations have not yet been investigated in detail due to the limitations in experimental procedures. Particle-based numerical methods discussed in the Section 3 of this paper have significant potential to be employed through computational microfluidics to better understand such phenomena efficiently. According to the evidence discussed throughout Section 3, it can be deduced that coupled approaches such as SPH-CG, SPH-DEM or LB-IB-DEM could potentially be used to simulate different components of a floating liquid marble system. The potential numerical methods for simulating different floating-liquid-marble components are given in the Table 3 below.

Table 3 Potentially suitable numerical methods to simulate different components of a floating liquid marble system

Component of a floating liquid marble system	**Potentially suitable numerical method**
Core liquid	SPH or LBM
Marble shell	CG or DEM
Carrier liquid	SPH or LBM
Multiphase (e.g., solid, liquid and gas) interactions (i.e., solid-fluid and fluid-fluid)	For SPH, Lennard-Jones (LJ) interactions [61]. For LBM, the pseudopotential model and the free energy model (Section 3.3.1)

The predictions from numerical modelling could then be used to evaluate the effectiveness and efficiency of different experimental transport and trapping mechanisms for floating liquid

marbles. For instance, there is the possibility to assess different liquid marble propulsion methods through numerically representing the corresponding force-interactions such as thermally induced forces, magnetically induced forces and electrochemically induced forces in either a coupled SPH-CG or an LB-based computational approach. Such a study has the potential to save time and monetary resources compared to purely experimental approaches. In addition, the subsequent experimental outcomes could be utilised to further calibrate and strengthen the numerical simulations leading to increased accuracy of predictions. In other words, numerical modelling and experimental procedures could synergistically aid each other while producing effective and efficient technological advances in this sub-domain of engineering.

4.2. Modelling effective surface tension of a liquid marble

As discussed throughout this paper, surface tension is one of the most critical parameters (if not the most critical) of a liquid marble system that governs its overall behaviour. However, due to complex features, e.g., the presence of solid particles at the liquid-air interface, irregular particle distributions and heterogenous deformation, the variation of surface tension with other parameters has proven difficult to be determined accurately through experimental means. For instance, the relationship between the actual surface area and effective surface tension is difficult to be determined experimentally [20] although an enhanced understanding would be key to optimise the corresponding experimental procedures and subsequent applications. There are numerous variables in a liquid marble system that affect the surface tension: marble shell parameters (size, shape, particle distribution on the liquid marble surface, particle packing, interparticle forces between coating particles); capillary interactions; volume of the core liquid and apparent contact angle (Fig. 6).

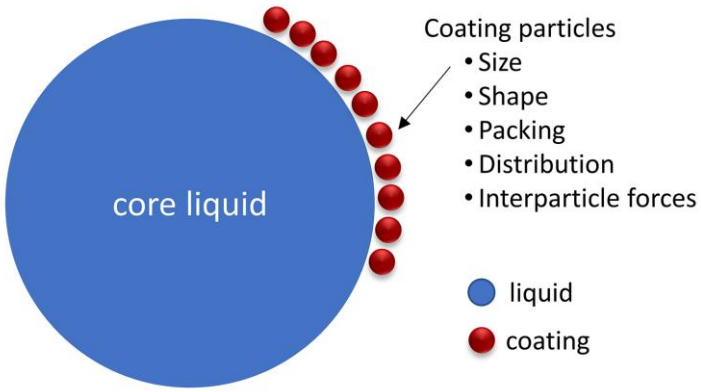

Fig. 6 Coating particle parameters influencing the effective surface tension of a liquid marble

Numerical modelling has the potential to address this gap in experimental studies. It can contribute to efficiently evaluate the influence of the aforementioned parameters on the surface tension of a liquid marble and its overall behaviour. Tartakovsky et al. [133, 134] have utilised an SPH-based numerical framework to effectively simulate surface tension in multiphase fluid flows that are affected by capillary interactions, contact angle and particle-particle interactions. Such an approach would have a significantly high relevance for liquid marbles. Furthermore, the particle-based SPH-DEM and SPH-CG plant cell modelling investigations by Van Liedekerke et al. [61], Karunasena et al. [34] and Rathnayaka et al. [64] have provided evidence that an equivalent numerical coupling could be adopted to evaluate the influence of the above parameters on the effective surface tension. Although these SPH-DEM and SPH-CG investigations did not specifically simulate surface tension with respect to plant cells, the underlying numerical framework clearly has the capability as demonstrated by multiphase flow study of Tartakovsky et al. [133, 134]. Another highlight of plant cell modelling is how it represents the influence of cell wall particles (membrane) and particle-particle interactions on the plant cell behaviour. An equivalent approach could potentially be adopted to simulate the effects of marble shell on critical liquid marble properties (e.g., surface tension and surface area). Establishing these relationships numerically would be able to address a critical gap in the current liquid marble experimental investigations while improving the efficacy of their real-world engineering applications.

In doing so, one of the possibilities is to calculate the surface tension forces acting on a liquid marble with the aid of the Young-Laplace equation,

$$p_s = \sigma\left(\frac{1}{r_1} + \frac{1}{r_2}\right) \tag{10}$$

where σ is the surface tension and r_1 and r_2 the principal radii of curvatures of a liquid marble [40]. In 2-D liquid marble models, it can be assumed that r_1 and r_2 are identical. Subsequently, the Young-Laplace pressure (p_s) acting on a liquid marble can be calculated as,

$$p_s = \frac{\sigma}{r} \tag{11}$$

where r is the radius of curvature of the liquid marble. Accordingly, the surface tension force ($\boldsymbol{F^s}$) can be calculated as,

$$\boldsymbol{F^s} = p_s A_p \tag{12}$$

where A_p is the equivalent area of a section of interest.

4.3. Coalescence of liquid marbles

As previously stated in this paper, the coalescence and splitting processes of liquid marbles are still not well understood [7]. Further insights would be useful for applications such as chemical and biological microreactors or micromixers where two or more liquid marbles containing different reagents or ingredients coalesce [12, 31]. There are dynamics of the kinetic energy to surface energy conversion (or vice versa) involved in these processes. The coalescence of liquid marbles, schematically represented in Fig. 7, requires sophisticated numerical modelling features to represent merging of liquid marbles through remodelling of the marble shells and union of the core liquid.

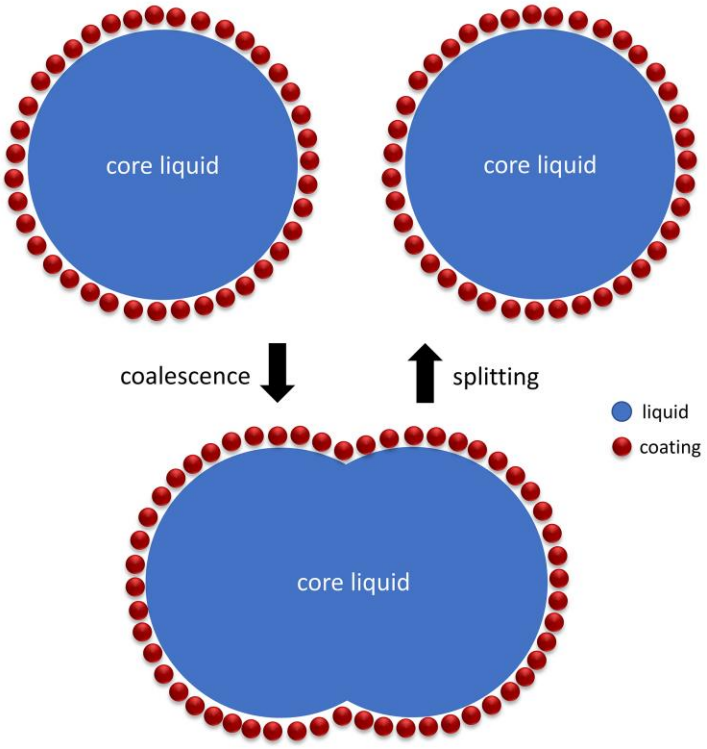

Fig. 7 Liquid marble coalescence (or splitting) process through merging and re-structuring of the core-liquid and marble shell components (or the reversal)

Among the particle-based methods discussed in this paper, CG-based approaches have the potential to simulate marble-shell dynamics during its remodelling process with respect to either coalescence or splitting. Simultaneously, either SPH or LBM could potentially be used to model core-liquid mechanics. An advantage of using a meshfree-based approach such as SPH or LBM would be the convenience of simulating the collisions and subsequent momentum transfer with respect to the coalescence process while representing the low-*Re* fluid flow characteristics effectively. The effects of fluid viscosity and interfacial tension could be assessed through such an approach. Moreover, depending on the necessity to explore the details

at the molecular scale in parallel to the solid and fluid dynamics of a liquid marble, relevant MD simulations could be implemented and coupled with either SPH, LBM or CG numerical methods. One of the concerns of such an approach would be the increased computational-and-time resource requirements to couple MD with either SPH, LBM or CG.

A successful numerical simulation would have the potential to facilitate precise prediction of key characteristics of the coalescence process. For instance, the time required to unify individual marbles, which would be a critical parameter to enable appropriate reaction-and-mixing rates [135]. In addition, it would be possible to approximate the subsequent morphological variations and micromechanical phenomena that are pivotal factors for the corresponding reactions and mixing processes [65]. Predictions from these modelling investigations could be used in the design of the actual liquid marble systems for coalescence. To the best of the authors' knowledge, such advanced numerical and computational analyses have not yet been reported in the scientific literature in the context of liquid marbles.

4.4. Morphology of the marble shell

The shell of a liquid marble is a combination of coating particles and pores that directly or indirectly prevents contact with the core liquid and the substrate (Fig. 8). The marble shell is a crucial component that determines the effective surface tension, robustness and elasticity of the overall liquid marble [136-138]. Different liquid marble applications exploit different properties of the marble shell such as its magnetic and electrical properties, thermal sensitivity, porosity and mechanical characteristics [20]. Accordingly, marble-shell morphology is a defining parameter for the overall liquid-marble behaviour. The marble-shell morphology has a mutual relationship with the behaviour of the core liquid as well as the carrying substrate. Despite the importance, only a few studies have so far been reported in the literature on morphological characteristics and structure of the marble shell [25, 139, 140]. These studies are mainly experimental whereas numerical modelling has the potential to address the critical phenomena related to the morphological behaviour of liquid marbles as given below.

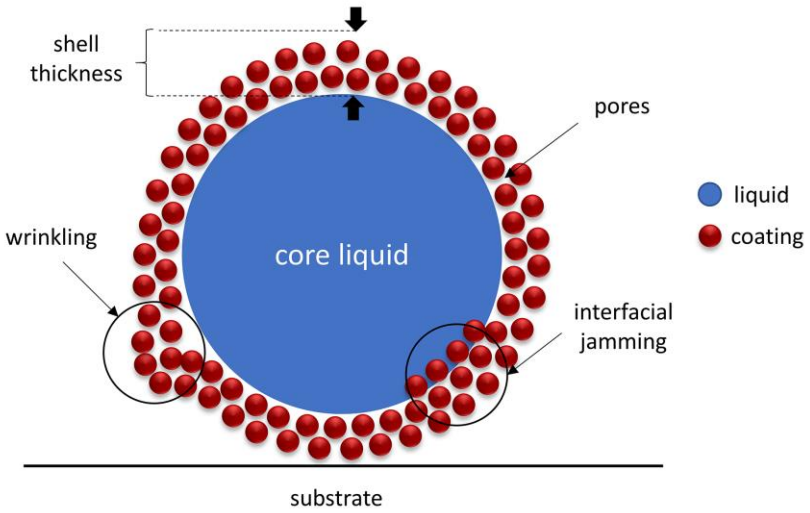

Fig. 8 Representation of some of the morphological characteristics of the marble shell that are crucial for determining the overall behaviour of a liquid marble

As discussed previously in this paper, surface tension of the core liquid is a crucial parameter that determines the overall performance of a liquid marble. Consequently, the morphological behaviour of the marble shell has a direct relationship with the core liquid surface tension. For instance, it has been found experimentally that the thickness and mass of a marble shell depends on the core liquid surface tension while giving rise to phenomena such as interfacial jamming, particle penetration and uneven coating particle distribution at the liquid-air interface [20]. A particle-based numerical approach can potentially be used to simulate these phenomena associated with the marble shell and the core liquid surface tension.

As discussed in the Section 4.2 of this paper, there is a significant potential for the effective surface tension of a liquid marble to be accurately predicted through a particle-based numerical approach, e.g., SPH-CG, SPH-DEM or LB-IB-DEM. The morphological behaviour of the marble shell can also be coupled to the same numerical representation efficiently in an analogous manner to the previously reported meshfree-based plant cell modelling studies [64, 141]. In those studies, the details of the cell-membrane wrinkling (Fig. 8) and subsequent interrelationships with core liquid evaporations (i.e., for the cell fluid) have been considered in detail. Such an approach also has the capability to simulate 3-D localised deformations of the marble shell. For example, surface wrinkling associated with applications such as floatation and coalescence. In addition, an SPH-CG approach can be used to simulate the surface area variation during different forms of manipulation along with the corresponding variations of surface tension, surface energy and kinetic energy, which are difficult parameters to be determined experimentally [35].

4.5. 3-D numerical modelling of liquid marbles

A 2-D model has limitations to accurately solve a problem which is naturally 3-D. Although the preliminary 2-D work by Polwaththe-Gallage et al. [40] provides innovative insights into numerical modelling of liquid marbles, it is still necessary to expand such numerical efforts up to the more realistic 3-D scale to reap the maximum benefits. To the best of authors' knowledge, there are no 3-D numerical modelling investigations of liquid marbles reported in the scientific literature so far. Nonetheless, there are ongoing efforts by the authors of this paper to develop a 3-D numerical model using a CG-based approach. Inspired by the fundamental CG-based 2-D numerical modelling work conducted by Polwaththe-Gallage et al. [40], these efforts aim to investigate the morphological behaviour of liquid marbles in detail. Fig. 9 provides a preliminary visualisation of the current results from the ongoing computational studies. Even though this work is still ongoing and unpublished, it provides an indication towards the possibility of more realistic 3-D computational modelling to be implemented in the context of liquid marbles through a CG-based approach.

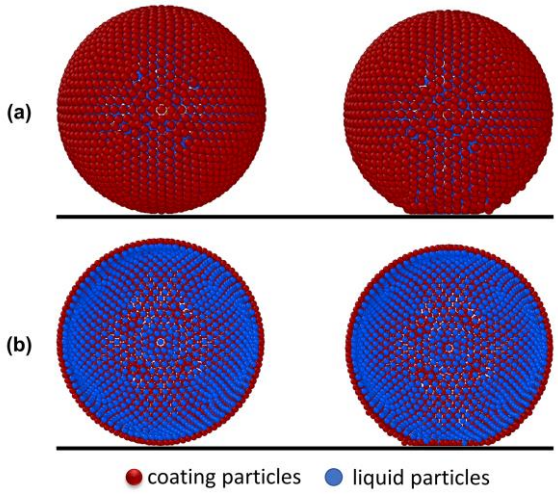

Fig. 9 Preliminary results (unpublished) from currently ongoing 3-D liquid marble numerical modelling studies by the authors of this paper: (a) External view; (b) Cross sectional view

5. Concluding remarks

Although numerous experimental and analytical research investigations have been conducted for studying liquid marble characteristics, numerical modelling investigations in this scope are extremely limited. Numerical modelling approaches can be used to improve the understanding of the physical behaviour of liquid marbles, and to overcome the use of time- and cost-intensive experimental-only procedures. Numerical modelling approaches can also contribute to analysing the 3-D morphological behaviour and subsequent dynamics of liquid marbles with

increased convenience and accuracy. This could increase the effectiveness and efficiency of liquid marble experimental investigations with respect to a myriad of engineering applications. Advanced particle-based numerical modelling techniques such as Smoothed Particle Hydrodynamics (SPH)-based approaches, Coarse-Grained (CG)-based approaches, and Lattice Boltzmann Method (LBM)-based approaches exhibit promising capabilities to simulate complex and multiphase physics involved with liquid marbles. Moreover, SPH- and CG-based numerical approaches have already been applied to model physical phenomena relevant to either liquid marbles or soft matter that closely resemble liquid marbles. The most appropriate particle-based numerical method to be used for a given application would depend on a number of criteria: *a)* the time scale of the problem; *b)* the spatial scale of the problem; *c)* the specific components of the system to be modelled (e.g., core liquid, marble shell, carrying fluid, substrate etc.); *d)* the nature of the physical behaviours to be modelled (e.g., floating, coalescence, micromechanics etc.); and *e)* other problem-specific conditions. New knowledge derived through these numerical studies has the potential to inspire new experiments while leading to impactful discoveries in this contemporary domain of research.

References

1. Bormashenko, E., *Liquid marbles: Properties and applications.* Current Opinion in Colloid & Interface Science, 2011. **16**(4): p. 266-271. https://doi.org/10.1016/j.cocis.2010.12.002
2. Asare-Asher, S., J.N. Connor, and R. Sedev, *Elasticity of liquid marbles.* Journal of colloid and interface science, 2015. **449**: p. 341-346.
3. Janardan, N., M.V. Panchagnula, and E. Bormashenko, *Liquid marbles: Physics and applications.* Sadhana, 2015. **40**(3): p. 653-671.
4. Ooi, C.H., R. Vadivelu, J. Jin, K.R. Sreejith, P. Singha, N.-K. Nguyen, and N.-T. Nguyen, *Liquid marble-based digital microfluidics – fundamentals and applications.* Lab on a Chip, 2021. **21**(7): p. 1199-1216. 10.1039/D0LC01290D
5. Nguyen, N.-T., *Micro Elastofluidics: Elasticity and Flexibility for Efficient Microscale Liquid Handling.* Micromachines, 2020. **11**(11). 10.3390/mi11111004
6. Aussillous, P. and D. Quéré, *Liquid marbles.* Nature, 2001. **411**(6840): p. 924-927. 10.1038/35082026
7. Jing, J. and N.-T. Nguyen, *Manipulation schemes and applications of liquid marbles for micro total analysis systems.* Microelectronic Engineering, 2018. **197**: p. 87-95.
8. Fujii, S., S. Kameyama, S.P. Armes, D. Dupin, M. Suzaki, and Y. Nakamura, *pH-responsive liquid marbles stabilized with poly (2-vinylpyridine) particles.* Soft Matter, 2010. **6**(3): p. 635-640.
9. Zhao, Y., Z. Xu, M. Parhizkar, J. Fang, X. Wang, and T. Lin, *Magnetic liquid marbles, their manipulation and application in optical probing.* Microfluidics and Nanofluidics, 2012. **13**(4): p. 555-564. 10.1007/s10404-012-0976-9
10. Vadivelu, R.K., C.H. Ooi, R.-Q. Yao, et al., *Generation of three-dimensional multiple spheroid model of olfactory ensheathing cells using floating liquid marbles.* Scientific Reports, 2015. **5**(1): p. 15083. 10.1038/srep15083

11. Tian, J., T. Arbatan, X. Li, and W. Shen, *Porous liquid marble shell offers possibilities for gas detection and gas reactions.* Chemical Engineering Journal, 2010. **15**: p. 347-353.
12. Xue, Y., H. Wang, Y. Zhao, L. Dai, L. Feng, X. Wang, and T. Lin, *Magnetic Liquid Marbles: A "Precise" Miniature Reactor.* Adv. Mater., 2010. **22**: p. 4814-4818.
13. Rong, X., R. Ettelaie, S.V. Lishchuk, H. Cheng, N. Zhao, F. Xiao, F. Cheng, and H. Yang, *Liquid marble-derived solid-liquid hybrid superparticles for CO2 capture.* Nature Communications, 2019. **10**(1): p. 1854. 10.1038/s41467-019-09805-7
14. Bormashenko, E. and A. Musin, *Revealing of water surface pollution with liquid marbles.* Applied Surface Science, 2009. **255**(12): p. 6429 - 6431.
15. Jin, J., C.H. Ooi, K.R. Sreejith, D.V. Dao, and N.-T. Nguyen, *Dielectrophoretic Trapping of a Floating Liquid Marble.* Physical Review Applied, 2019. **11**(4): p. 044059. 10.1103/PhysRevApplied.11.044059
16. Sreejith, K.R., L. Gorgannezhad, J. Jin, et al., *Core-Shell Beads Made by Composite Liquid Marble Technology as A Versatile Microreactor for Polymerase Chain Reaction.* Micromachines, 2020. **11**(3). 10.3390/mi11030242
17. Roy, P.K., B.P. Binks, S. Fujii, S. Shoval, and E. Bormashenko, *Composite Liquid Marbles as a Macroscopic Model System Representing Shedding of Enveloped Viruses.* The Journal of Physical Chemistry Letters, 2020. **11**(11): p. 4279-4285. 10.1021/acs.jpclett.0c01230
18. Roy, P.K., B.P. Binks, E. Bormashenko, I. Legchenkova, S. Fujii, and S. Shoval, *Manufacture and properties of composite liquid marbles.* Journal of Colloid and Interface Science, 2020. **575**: p. 35-41. https://doi.org/10.1016/j.jcis.2020.04.066
19. Ooi, C.H., R.K. Vadivelu, J. St John, D.V. Dao, and N.-T. Nguyen, *Deformation of a floating liquid marble.* Soft matter, 2015. **11**(23): p. 4576-4583.
20. Singha, P., N.-K. Nguyen, K.R. Sreejith, H. An, N.-T. Nguyen, and C.H. Ooi, *Effect of Core Liquid Surface Tension on the Liquid Marble Shell.* Advanced Materials Interfaces, 2020. **n/a**(n/a): p. 2001591. https://doi.org/10.1002/admi.202001591
21. McHale, G. and M. Newton, *Liquid marbles: topical context within soft matter and recent progress.* Soft Matter, 2015. **11**(13): p. 2530-2546.
22. Cengiz, U. and H.Y. Erbil, *The lifetime of floating liquid marbles: the influence of particle size and effective surface tension.* Soft Matter, 2013. **9**(37): p. 8980-8991. 10.1039/C3SM51304A
23. Bormashenko, E., *New insights into liquid marbles.* Soft Matter, 2012. **8**(43): p. 11018-11021. 10.1039/C2SM26189H
24. Nguyen, N.-T., *Deformation of Ferrofluid Marbles in the Presence of a Permanent Magnet.* Langmuir, 2013. **29**(45): p. 13982-13989. 10.1021/la4032859
25. Aussillous, P. and D. Quéré, *Properties of liquid marbles.* Proceedings of the Royal Society A: Mathematical, Physical and Engineering Sciences, 2006. **462**(2067): p. 973-999. 10.1098/rspa.2005.1581
26. Bormashenko, E., Y. Bormashenko, and G. Oleg, *On the nature of the friction between nonstick droplets and solid substrates.* Langmuir, 2010. **26**(15): p. 12479-12482.
27. Oliveira, N.M., R.L. Reis, and J.F. Mano, *The Potential of Liquid Marbles for Biomedical Applications: A Critical Review.* Advanced Healthcare Materials, 2017. **6**(19): p. 1700192. 10.1002/adhm.201700192
28. Liu, Z., X. Fu, B.P. Binks, and H.C. Shum, *Mechanical Compression to Characterize the Robustness of Liquid Marbles.* Langmuir, 2015. **31**(41): p. 11236-11242. 10.1021/acs.langmuir.5b02792
29. Singha, P., C.H. Ooi, N.-K. Nguyen, K.R. Sreejith, J. Jin, and N.-T. Nguyen, *Capillarity: revisiting the fundamentals of liquid marbles.* Microfluidics and Nanofluidics, 2020. **24**(10): p. 81. 10.1007/s10404-020-02385-9

30. Jin, J., K.R. Sreejith, C.H. Ooi, D.V. Dao, and N.-T. Nguyen, *Critical Trapping Conditions for Floating Liquid Marbles.* Physical Review Applied, 2020. **13**(1): p. 014002. 10.1103/PhysRevApplied.13.014002
31. Jing, J., C.H. Ooi, D.V. Dao, and N.-T. Nguyen, *Coalescence Processes of Droplets and Liquid Marbles.* Micromachines, 2017. **8**(11): p. 336.
32. Polwaththe-Gallage, H.-N., C.H. Ooi, J. Jin, E. Sauret, N.-T. Nguyen, Z. Li, and Y. Gu, *The stress-strain relationship of liquid marbles under compression.* Applied Physics Letters, 2019. **114**(4): p. 043701. 10.1063/1.5079438
33. Polwaththe-Gallage, H.-N., S.C. Saha, E. Sauret, R. Flower, and Y. Gu, *A coupled SPH-DEM approach to model the interactions between multiple red blood cells in motion in capillaries.* International Journal of Mechanics and Materials in Design, 2016. **12**(4): p. 477-494. 10.1007/s10999-015-9328-8
34. Karunasena, H., W. Senadeera, R.J. Brown, and Y.J.S.m. Gu, *A particle based model to simulate microscale morphological changes of plant tissues during drying.* Soft Matter, 2014. **10**(29): p. 5249-5268.
35. Rathnayaka, C.M., H.C.P. Karunasena, W. Senadeera, and Y.T. Gu, *Application of a coupled smoothed particle hydrodynamics (SPH) and coarse-grained (CG) numerical modelling approach to study three-dimensional (3-D) deformations of single cells of different food-plant materials during drying.* Soft Matter, 2018. **14**(11): p. 2015-2031. 10.1039/C7SM01465A
36. Rathnayaka, C.M., H.C.P. Karunasena, W. Senadeera, and Y.T. Gu, *Modelling 3-D cellular microfluidics of different plant cells for the prediction of cellular deformations under external mechanical compression: A SPH-CG-based computational study*, in *Proceedings of the 22nd Australasian Fluid Mechanics Conference AFMC2020*, H. Chanson and R. Brown, Editors. 2020, The University of Queensland: Brisbane, QLD Australia. 10.14264/1374f47
37. Ye, T., N. Phan-Thien, and C.T. Lim, *Particle-based simulations of red blood cells—A review.* Journal of Biomechanics, 2016. **49**(11): p. 2255-2266. https://doi.org/10.1016/j.jbiomech.2015.11.050
38. Mahadevan, L. and Y. Pomeau, *Rolling droplets.* Physics of Fluids, 1999. **11**(9): p. 2449-2453. 10.1063/1.870107
39. Wong, C.Y.H., M. Adda-Bedia, and D. Vella, *Non-wetting drops at liquid interfaces: from liquid marbles to Leidenfrost drops.* Soft Matter, 2017. **13**: p. 5250-5260.
40. Polwaththe-Gallage, H.-N., E. Sauret, N.-T. Nguyen, S.C. Saha, and Y. Gu, *A novel numerical model to predict the morphological behavior of magnetic liquid marbles using coarse grained molecular dynamics concepts.* Physics of Fluids, 2018. **30**(1): p. 017105. 10.1063/1.5000289
41. O'Connor, J., P. Day, P. Mandal, and A. Revell, *Computational fluid dynamics in the microcirculation and microfluidics: what role can the lattice Boltzmann method play?* Integrative Biology, 2016. **8**(5): p. 589-602.
42. Erickson, D., *Towards numerical prototyping of labs-on-chip: modeling for integrated microfluidic devices.* Microfluidics and Nanofluidics, 2005. **1**(4): p. 301-318.
43. Liu, Y. and W.K. Liu, *Rheology of red blood cell aggregation by computer simulation.* Journal of Computational Physics, 2006. **220**(1): p. 139-154.
44. Tsubota, K.I., S. Wada, H. Kamada, Y. Kitagawa, R. Lima, and T. Yamaguchi, *A Particle Method for Blood Flow Simulation: Application to Flowing Red Blood Cells and Platelets.* Journal of the Earth Simulator, 2006. **5**: p. 2-7.
45. Schaller, V., G. Wahnström, A. Sanz-Velasco, P. Enoksson, and C. Johansson, *Monte Carlo simulation of magnetic multi-core nanoparticles.* Journal of Magnetism and Magnetic Materials, 2009. **321**(10): p. 1400-1403.
46. Wang, Z., C. Holm, and H.W. Müller, *Molecular dynamics study on the equilibrium magnetization properties and structure of ferrofluids.* Physical Review E, 2002. **66**: p. 1-13.

47. Vogiatzis, G.G. and D.N. Theodorou, *Multiscale Molecular Simulations of Polymer-Matrix Nanocomposites.* Archives of Computational Methods in Engineering, 2018. **25**(3): p. 591-645. 10.1007/s11831-016-9207-y

48. Perilla, J. and K. Schulten, *Physical properties of the HIV-1 capsid from all-atom molecular dynamics simulations.* Nature communications, 2017. **8**: p. 15959-15959.

49. Liu, M. and G. Liu, *Smoothed particle hydrodynamics (SPH): an overview and recent developments.* Archives of computational methods in engineering, 2010. **17**(1): p. 25-76.

50. Liu, G.-R. and M. Liu, *Smoothed particle hydrodynamics: a meshfree particle method*. 2003: World Scientific.

51. Liu, W.K., Y. Chen, S. Jun, J.S. Chen, T. Belytschko, C. Pan, R.A. Uras, and C.T. Chang, *Overview and applications of the reproducing Kernel Particle methods.* Archives of Computational Methods in Engineering, 1996. **3**(1): p. 3-80. 10.1007/BF02736130

52. Frank, X. and P. Perré, *The Potential of Meshless Methods to Address Physical and Mechanical Phenomena Involved during Drying at the Pore Level.* Drying Technology, 2010. **28**(8): p. 932-943. 10.1080/07373937.2010.497077

53. Perré, P., *A review of modern computational and experimental tools relevant to the field of drying.* Drying Technology, 2011. **29**(13): p. 1529-1541.

54. Morris, J.P., P.J. Fox, and Y. Zhu, *Modeling Low Reynolds Number Incompressible Flows Using SPH.* Journal of Computational Physics, 1997. **136**(1): p. 214-226. http://dx.doi.org/10.1006/jcph.1997.5776

55. Van Liedekerke, P., P. Ghysels, E. Tijskens, G. Samaey, D. Roose, and H. Ramon, *Mechanisms of soft cellular tissue bruising. A particle based simulation approach.* Soft Matter, 2011. **7**(7): p. 3580-3591.

56. Wijerathne, W.D.C.C., C.M. Rathnayaka, H.C.P. Karunasena, W. Senadeera, E. Sauret, I.W. Turner, and Y.T. Gu, *A coarse-grained multiscale model to simulate morphological changes of food-plant tissues undergoing drying.* Soft Matter, 2019. **15**(5): p. 901-916. 10.1039/C8SM01593G

57. Rafiee, A., M.T. Manzari, and M. Hosseini, *An incompressible SPH method for simulation of unsteady viscoelastic free-surface flows.* International Journal of Non-Linear Mechanics, 2007. **42**(10): p. 1210-1223. https://doi.org/10.1016/j.ijnonlinmec.2007.09.006

58. Hérault, A., G. Bilotta, A. Vicari, E. Rustico, and C. Del Negro, *Numerical simulation of lava flow using a GPU SPH model.* Annals of Geophysics; Vol 54, No 5 (2011): The lava flow invasion hazard map at Mount Etna and methods for its dynamic updateDO - 10.4401/ag-5343, 2011.

59. Liu, M.B., G.R. Liu, L.W. Zhou, and J.Z. Chang, *Dissipative Particle Dynamics (DPD): An Overview and Recent Developments.* Archives of Computational Methods in Engineering, 2015. **22**(4): p. 529-556. 10.1007/s11831-014-9124-x

60. Van Liedekerke, P., P. Ghysels, E. Tijskens, G. Samaey, B. Smeedts, D. Roose, and H. Ramon, *A particle-based model to simulate the micromechanics of single-plant parenchyma cells and aggregates.* Physical Biology, 2010. **7**(2): p. 026006.

61. Van Liedekerke, P., E. Tijskens, H. Ramon, P. Ghysels, G. Samaey, and D. Roose, *Particle-based model to simulate the micromechanics of biological cells.* Physical Review E, 2010. **81**(6): p. 061906.

62. Rathnayaka, C.M., H.C.P. Karunasena, Y.T. Gu, L. Guan, and W. Senadeera, *Novel trends in numerical modelling of plant food tissues and their morphological changes during drying – A review.* Journal of Food Engineering, 2017. **194**: p. 24-39. http://dx.doi.org/10.1016/j.jfoodeng.2016.09.002

63. Karunasena, H.C.P., W. Senadeera, R.J. Brown, and Y.T. Gu, *Simulation of plant cell shrinkage during drying – A SPH–DEM approach.* Engineering Analysis with Boundary Elements, 2014. **44**(0): p. 1-18. http://dx.doi.org/10.1016/j.enganabound.2014.04.004

64. Rathnayaka, C.M., H.C.P. Karunasena, W. Senadeera, H.N. Polwaththe-Gallage, and Y.T. Gu, *A 3-D coupled Smoothed Particle Hydrodynamics and Coarse-Grained model to simulate drying mechanisms of small cell aggregates.* Applied Mathematical Modelling, 2019. **67**: p. 219-233. https://doi.org/10.1016/j.apm.2018.09.037

65. Rathnayaka, C.M., H.C.P. Karunasena, W. Wijerathne, W. Senadeera, and Y.T. Gu, *A three-dimensional (3-D) meshfree-based computational model to investigate stress-strain-time relationships of plant cells during drying.* PLoS One, 2020. **15**(7): p. e0235712. 10.1371/journal.pone.0235712

66. Rathnayaka, C.M., H.C.P. Karunasena, Y.T. Gu, L. Guan, J. Banks, and W. Senadeera, *A 3-D meshfree numerical model to analyze cellular scale shrinkage of different categories of fruits and vegetables during drying*, in *The 7th International Conference on Computational Methods*, G.R. Liu and S. Li, Editors. 2016, Scientech Publisher: Berkeley, CA, USA. p. 1070-1080.

67. Polwaththe-Gallage, H.-N., S.C. Saha, E. Sauret, R. Flower, and Y. Gu, *Numerical Investigation of Motion and Deformation of a Single Red Blood Cell in a Stenosed Capillary.* International Journal of Computational Methods, 2015. **12**(04): p. 1540003.

68. Wu, T. and J.J. Feng, *Simulation of malaria-infected red blood cells in microfluidic channels: Passage and blockage.* Biomicrofluidics, 2013. **7**(4): p. 044115. 10.1063/1.4817959

69. Polwaththe-Gallage, H.-N., S.C. Saha, E. Sauret, R. Flower, W. Senadeera, and Y. Gu, *SPH-DEM approach to numerically simulate the deformation of three-dimensional RBCs in non-uniform capillaries.* BioMedical Engineering OnLine, 2016. **15**(2): p. 161. 10.1186/s12938-016-0256-0

70. Crespo, A.C., J.M. Dominguez, A. Barreiro, M. Gómez-Gesteira, and B.D. Rogers, *GPUs, a New Tool of Acceleration in CFD: Efficiency and Reliability on Smoothed Particle Hydrodynamics Methods.* PLOS ONE, 2011. **6**(6): p. e20685. 10.1371/journal.pone.0020685

71. Hérault, A., G. Bilotta, and R.A. Dalrymple, *SPH on GPU with CUDA.* Journal of Hydraulic Research, 2010. **48**(sup1): p. 74-79. 10.1080/00221686.2010.9641247

72. Winkler, D., M. Rezavand, and W. Rauch, *Neighbour lists for smoothed particle hydrodynamics on GPUs.* Computer Physics Communications, 2018. **225**: p. 140-148. https://doi.org/10.1016/j.cpc.2017.12.014

73. Jin, J. and N.-T. Nguyen, *Manipulation schemes and applications of liquid marbles for micro total analysis systems.* Microelectronic Engineering, 2018. **197**: p. 87-95. https://doi.org/10.1016/j.mee.2018.06.003

74. Li, H. and G. Lykotrafitis, *Two-component coarse-grained molecular-dynamics model for the human erythrocyte membrane*. Biophysical Journal, 2012. **102**(1): p. 75-84. 10.1016/j.bpj.2011.11.4012

75. Jiang, L.-G., H.-A. Wu, X.-Z. Zhou, and X.-X. Wang, *Coarse-grained molecular dynamics simulation of a red blood cell.* Chinese Physics Letters, 2010. **27**(2). 10.1088/0256-307x/27/2/028704

76. Lyu, J., P.G. Chen, G. Boedec, M. Leonetti, and M. Jaeger, *Hybrid continuum–coarse-grained modeling of erythrocytes.* Comptes Rendus Mécanique, 2018. **346**(6): p. 439-448. https://doi.org/10.1016/j.crme.2018.04.015

77. Pivkin, I.V. and G.E. Karniadakis, *Accurate coarse-grained modeling of red blood cells.* Physical Review Letters, 2008. **101**(11). 10.1103/PhysRevLett.101.118105

78. Fedosov, D.A., B. Caswell, and G.E. Karniadakis. *Coarse-grained red blood cell model with accurate mechanical properties, rheology and dynamics*. in *Annual International Conference of the IEEE Engineering in Medicine and Biology Society*. 2009. Minneapolis, MN, USA IEEE.

79. Hale, J.P., G. Marcelli, K.H. Parker, C.P. Winlove, and P.G. Petrov, *Red blood cell thermal fluctuations: comparison between experiment and molecular dynamics simulations.* Soft Matter, 2009. **5**(19): p. 3603-3606. 10.1039/b910422d

80. Li, H. and G. Lykotrafitis, *Erythrocyte membrane model with explicit description of the lipid bilayer and the spectrin network.* Biophysical Journal, 2014. **107**(3): p. 642-653. http://dx.doi.org/10.1016/j.bpj.2014.06.031

81. Li, X., Z. Peng, H. Lei, M. Dao, and G.E. Karniadakis, *Probing red blood cell mechanics, rheology and dynamics with a two-component multi-scale model.* Philosophical Transactions of the Royal Society A: Mathematical, Physical and Engineering Sciences, 2014. **372**.

82. Kim, D.-H., B. Li, F. Si, J.M. Phillip, D. Wirtz, and S.X. Sun, *Volume regulation and shape bifurcation in the cell nucleus.* J Cell Sci, 2015. **128**(18): p. 3375-3385.

83. Lykov, K., X. Li, H. Lei, I.V. Pivkin, and G.E. Karniadakis, *Inflow/outflow boundary conditions for particle-based blood flow simulations: Application to arterial bifurcations and trees.* PLoS Computational Biology, 2015. **11**(8). 10.1371/journal.pcbi.1004410

84. Chang, H.-Y., X. Li, H. Li, and G.E. Karniadakis, *MD/DPD Multiscale Framework for Predicting Morphology and Stresses of Red Blood Cells in Health and Disease.* PLoS Computational Biology, 2016. **12**(10). 10.1371/journal.pcbi.1005173

85. Barns, S., M.A. Balanant, E. Sauret, R. Flower, S. Saha, and Y. Gu, *Investigation of red blood cell mechanical properties using AFM indentation and coarse-grained particle method.* Biomedical Engineeing Online, 2017. **16**(1). 10.1186/s12938-017-0429-5

86. Tang, Y.-H., L. Lu, H. Li, C. Evangelinos, L. Grinberg, V. Sachdeva, and G.E. Karniadakis, *OpenRBC: A fast simulator of red blood cells at protein resolution.* Biophysical Journal, 2017. **112**(10): p. 2030-2037. http://dx.doi.org/10.1016/j.bpj.2017.04.020

87. Li, H., L. Lu, X. Li, P.A. Buffet, M. Dao, G.E. Karniadakis, and S. Suresh, *Mechanics of diseased red blood cells in human spleen and consequences for hereditary blood disorders.* Proceedings of the National Academy of Sciences of the United States of America, 2018. **115**(38): p. 9574-9579. 10.1073/pnas.1806501115

88. Geekiyanage, N.M., M.A. Balanant, E. Sauret, S. Saha, R. Flower, C.T. Lim, and Y. Gu, *A coarse-grained red blood cell membrane model to study stomatocyte-discocyte-echinocyte morphologies.* PLoS ONE, 2019. **14**(4). 10.1371/journal.pone.0215447

89. Geekiyanage, N.M., E. Sauret, S.C. Saha, R.L. Flower, and Y.T. Gu, *Deformation behaviour of stomatocyte, discocyte and echinocyte red blood cell morphologies during optical tweezers stretching.* Biomechanics and Modeling in Mechanobiology, 2020. **19**(5): p. 1827-1843. 10.1007/s10237-020-01311-w

90. Geekiyanage, N., E. Sauret, S. Saha, R. Flower, and Y. Gu, *Modelling of Red Blood Cell Morphological and Deformability Changes during In-Vitro Storage.* Applied Sciences, 2020. **10**(9). 10.3390/app10093209

91. Mukhopadhyay, R., G. Lim, and M. Wortis, *Echinocyte shapes: Bending, stretching, and shear determine spicule shape and spacing.* Biophysical Journal, 2002. **82**(4): p. 1756-1772.

92. Marcelli, G., K.H. Parker, and C.P. Winlove, *Thermal fluctuations of red blood cell membrane via a constant-area particle-dynamics model.* Biophysical Journal, 2005. **89**(4): p. 2473-2480. 10.1529/biophysj.104.056168

93. Li, X., H. Li, H.-Y. Chang, G. Lykotrafitis, and G.E. Karniadakis, *Computational biomechanics of human red blood cells in hematological disorders.* Journal of Biomechanical Engineering, 2017. **139**(2). 10.1115/1.4035120

94. Fedosov, D.A., B. Caswell, and G.E. Karniadakis, *Systematic coarse-graining of spectrin-level red blood cell models.* Computer Methods in Applied Mechanics and Engineering, 2010. **199**(29–32): p. 1937-1948. http://dx.doi.org/10.1016/j.cma.2010.02.001

95. Succi, S., *Lattice Boltzmann 2038.* EPL (Europhysics Letters), 2015. **109**(5): p. 50001. 10.1209/0295-5075/109/50001

96. Shan, X., X.-F. Yuan, and H. Chen, *Kinetic theory representation of hydrodynamics: a way beyond the Navier–Stokes equation.* Journal of Fluid Mechanics, 2006. **550**: p. 413-441. 10.1017/S0022112005008153

97. Zhang, J., *Lattice Boltzmann method for microfluidics: models and applications.* Microfluidics and Nanofluidics, 2011. **10**: p. 1-28.

98. Obrecht, C., F. Kuznik, B. Tourancheau, and J.-J. Roux, *Multi-GPU implementation of the lattice Boltzmann method.* Computers & Mathematics with Applications, 2013. **65**(2): p. 252-261.

99. Bernaschi, M., S. Melchionna, and S. Succi, *Mesoscopic simulations at the physics-chemistry-biology interface.* Reviews of Modern Physics, 2019. **91**(2): p. 025004. 10.1103/RevModPhys.91.025004

100. Meng, J., Y. Zhang, and X. Shan, *Multiscale lattice Boltzmann approach to modeling gas flows.* Physical Review E, 2011. **83**(4): p. 046701.

101. Chacon, L., G. Chen, D.A. Knoll, C. Newman, H. Park, W. Taitano, J.A. Willert, and G. Womeldorff, *Multiscale high-order/low-order (HOLO) algorithms and applications.* Journal of Computational Physics, 2017. **330**: p. 21-45.

102. Wang, M. and S. Chen, *Multiscale simulations.* Encyclopedia of Microfluidics and Nanofluidics, 2015: p. 2326-2334.

103. Liu, X., Y.-F. Zhu, B. Gong, J.-P. Yu, and S.-T. Cui, *From molecular dynamics to lattice Boltzmann: a new approach for pore-scale modeling of multi-phase flow.* Petroleum Science, 2015. **12**(2): p. 282-292.

104. Krüger, T., H. Kusumaatmaja, A. Kuzmin, O. Shardt, G. Silva, and E.M.J.S.I.P. Viggen, *The lattice Boltzmann method*. Vol. 10. 2017. 4-15.

105. Succi, S. and S. Succi, *The Lattice Boltzmann Equation: For Complex States of Flowing Matter*. 2018: Oxford University Press.

106. Van den Akker, H.E.A., *Lattice Boltzmann simulations for multi-scale chemical engineering.* Current Opinion in Chemical Engineering, 2018. **21**: p. 67-75. https://doi.org/10.1016/j.coche.2018.03.003

107. Zhang, J., B. Li, and D.Y. Kwok, *Mean-field free-energy approach to the lattice Boltzmann method for liquid-vapor and solid-fluid interfaces.* Physical Review E, 2004. **69**(3): p. 032602. 10.1103/PhysRevE.69.032602

108. Gunstensen, A.K., D.H. Rothman, S. Zaleski, and G. Zanetti, *Lattice Boltzmann model of immiscible fluids.* Physical Review A, 1991. **43**(8): p. 4320-4327. 10.1103/PhysRevA.43.4320

109. Shan, X. and H. Chen, *Lattice Boltzmann model for simulating flows with multiple phases and components.* Physical Review E, 1993. **47**(3): p. 1815-1819. 10.1103/PhysRevE.47.1815

110. Li, Q., K.H. Luo, Q.J. Kang, Y.L. He, Q. Chen, and Q. Liu, *Lattice Boltzmann methods for multiphase flow and phase-change heat transfer*. Progress in Energy and Combustion Science, 2016. **52**: p. 62-105. https://doi.org/10.1016/j.pecs.2015.10.001

111. From, C.S., E. Sauret, S.A. Galindo-Torres, and Y.T. Gu, *Interaction pressure tensor on high-order lattice Boltzmann models for nonideal fluids.* Physical Review E, 2019. **99**(6): p. 063318. 10.1103/PhysRevE.99.063318

112. From, C.S., E. Sauret, S.A. Galindo-Torres, and Y.T. Gu, *Application of high-order lattice Boltzmann pseudopotential models.* Physical Review E, 2020. **101**(3): p. 033303. 10.1103/PhysRevE.101.033303

113. Falcucci, G., G. Bella, G. Chiatti, S. Chibbaro, M. Sbragaglia, and S. Succi, *Lattice Boltzmann models with mid-range interactions.* Communications in Computational Physics, 2007. **2**(6): p. 1071-1084.

114. Lulli, M., R. Benzi, and M. Sbragaglia, *Metastability at the Yield-Stress Transition in Soft Glasses.* Physical Review X, 2018. **8**(2): p. 021031. 10.1103/PhysRevX.8.021031

115. Dollet, B., A. Scagliarini, and M. Sbragaglia, *Two-dimensional plastic flow of foams and emulsions in a channel: experiments and lattice Boltzmann simulations.* Journal of Fluid Mechanics, 2015. **766**: p. 556-589. 10.1017/jfm.2015.28

116. Liu, X., P. Cheng, and X. Quan, *Lattice Boltzmann simulations for self-propelled jumping of droplets after coalescence on a superhydrophobic surface.* International Journal of Heat and Mass Transfer, 2014. **73**: p. 195-200. https://doi.org/10.1016/j.ijheatmasstransfer.2014.01.060

117. Peng, B., S. Wang, Z. Lan, W. Xu, R. Wen, and X. Ma, *Analysis of droplet jumping phenomenon with lattice Boltzmann simulation of droplet coalescence.* Applied Physics Letters, 2013. **102**(15): p. 151601. 10.1063/1.4799650

118. Benzi, R., L. Biferale, M. Sbragaglia, S. Succi, and F. Toschi, *Mesoscopic modeling of a two-phase flow in the presence of boundaries: The contact angle.* Physical Review E, 2006. **74**(2): p. 021509. 10.1103/PhysRevE.74.021509

119. Hyväluoma, J. and J. Harting, *Slip Flow Over Structured Surfaces with Entrapped Microbubbles.* Physical Review Letters, 2008. **100**(24): p. 246001. 10.1103/PhysRevLett.100.246001

120. Hyväluoma, J., A. Koponen, P. Raiskinmäki, and J. Timonen, *Droplets on inclined rough surfaces.* The European Physical Journal E, 2007. **23**(3): p. 289-293. 10.1140/epje/i2007-10190-7

121. Varagnolo, S., D. Ferraro, P. Fantinel, M. Pierno, G. Mistura, G. Amati, L. Biferale, and M. Sbragaglia, *Stick-Slip Sliding of Water Drops on Chemically Heterogeneous Surfaces.* Physical Review Letters, 2013. **111**(6): p. 066101. 10.1103/PhysRevLett.111.066101

122. Varagnolo, S., V. Schiocchet, D. Ferraro, M. Pierno, G. Mistura, M. Sbragaglia, A. Gupta, and G. Amati, *Tuning Drop Motion by Chemical Patterning of Surfaces.* Langmuir, 2014. **30**(9): p. 2401-2409. 10.1021/la404502g

123. Falcucci, G., E. Jannelli, S. Ubertini, and S. Succi, *Direct numerical evidence of stress-induced cavitation.* Journal of Fluid Mechanics, 2013. **728**: p. 362-375. http://dx.doi.org/10.1017/jfm.2013.271

124. Sadullah, M.S., G. Launay, J. Parle, R. Ledesma-Aguilar, Y. Gizaw, G. McHale, G.G. Wells, and H. Kusumaatmaja, *Bidirectional motion of droplets on gradient liquid infused surfaces.* Communications Physics, 2020. **3**(1): p. 166. 10.1038/s42005-020-00429-8

125. Panter, J.R., Y. Gizaw, and H. Kusumaatmaja, *Multifaceted design optimization for superomniphobic surfaces.* Science Advances, 2019. **5**(6): p. eaav7328. 10.1126/sciadv.aav7328

126. De Haan, M., G. Zavodszky, V. Azizi, and A.G. Hoekstra, *Numerical Investigation of the Effects of Red Blood Cell Cytoplasmic Viscosity Contrasts on Single Cell and Bulk Transport Behaviour*. 2018. **8**(9): p. 1616.

127. Závodszky, G., B. van Rooij, B. Czaja, V. Azizi, D. de Kanter, and A.G. Hoekstra, *Red blood cell and platelet diffusivity and margination in the presence of cross-stream gradients in blood flows.* Physics of Fluids, 2019. **31**(3): p. 031903. 10.1063/1.5085881

128. Karunasena, H.C.P., Y.T. Gu, R.J. Brown, and W. Senadeera, *Numerical investigation of plant tissue porosity and its influence on cellular level shrinkage during drying.* Biosystems Engineering, 2015. **132**(0): p. 71-87. http://dx.doi.org/10.1016/j.biosystemseng.2015.02.002

129. Rathnayaka, C.M., H.C.P. Karunasena, W. Senadeera, L. Guan, and Y.T. Gu, *Three-Dimensional (3D) Numerical Modeling of Morphogenesis in Dehydrated Fruits and Vegetables*, in *Advances in Agricultural Machinery and Technologies*, G. Chen, Editor. 2018, CRC Press: Boca Raton. p. 431-454.

130. Sauret, E., S. Galindo Torres, S. Kuruneru, P. Zhang, S. Saha, and Y. Gu, *Comparison between FVM-DEM & LBM-DEMof particle-laden flows in idealised porous metal foam heat exchangers*, in *18th IAHR Conference on Wet Cooling Towers and Air Cooled Heat Exchangers, 16-20 October 2017, Lyon, France*. 2017.

131. Galindo-Torres, S.A., A. Scheuermann, L. Li, D.M. Pedroso, and D.J. Williams, *A Lattice Boltzmann model for studying transient effects during imbibition–drainage cycles in unsaturated soils.* Computer Physics Communications, 2013. **184**(4): p. 1086-1093. https://doi.org/10.1016/j.cpc.2012.11.015

132. Ohno, S., Y. Tsuda, K. Nakai, S. Fujii, Y. Nakamura, and S.-i. Yusa, *pH-responsive Liquid Marbles Prepared Using Fluorinated Fatty Acid.* Chemistry Letters, 2016. **45**(5): p. 547-549. 10.1246/cl.160056

133. Tartakovsky, A. and P. Meakin, *Modeling of surface tension and contact angles with smoothed particle hydrodynamics.* Physical Review E, 2005. **72**(2): p. 026301. 10.1103/PhysRevE.72.026301

134. Tartakovsky, A.M., P. Meakin, and A.L. Ward, *Smoothed particle hydrodynamics model of non-aqueous phase liquid flow and dissolution.* Transport in Porous Media, 2009. **76**(1): p. 11-34.

135. Mohammadi, M., S. Shahhosseini, and M. Bayat, *Direct numerical simulation of water droplet coalescence in the oil.* International Journal of Heat and Fluid Flow, 2012. **36**: p. 58-71. https://doi.org/10.1016/j.ijheatfluidflow.2012.04.001

136. Zang, D., Z. Chen, Y. Zhang, K. Lin, X. Geng, and B.P. Binks, *Effect of particle hydrophobicity on the properties of liquid water marbles.* Soft Matter, 2013. **9**(20): p. 5067-5073. 10.1039/C3SM50421B

137. Bhosale, P.S., M.V. Panchagnula, and H.A. Stretz, *Mechanically robust nanoparticle stabilized transparent liquid marbles.* Applied Physics Letters, 2008. **93**(3): p. 034109. 10.1063/1.2959853

138. Rendos, A., N. Alsharif, B.L. Kim, and K.A. Brown, *Elasticity and failure of liquid marbles: influence of particle coating and marble volume.* Soft Matter, 2017. **13**(47): p. 8903-8909. 10.1039/C7SM01676J

139. Nguyen, T.H., W. Shen, and K. Hapgood, *Effect of formulation hydrophobicity on drug distribution in wet granulation.* Chemical Engineering Journal, 2010. **164**(2): p. 330-339. https://doi.org/10.1016/j.cej.2010.05.008

140. Bormashenko, E., R. Pogreb, G. Whyman, A. Musin, Y. Bormashenko, and Z. Barkay, *Shape, Vibrations, and Effective Surface Tension of Water Marbles.* Langmuir, 2009. **25**(4): p. 1893-1896. 10.1021/la8028484

141. Karunasena, H.C.P., R.J. Brown, Y.T. Gu, and W. Senadeera, *Application of meshfree methods to numerically simulate microscale deformations of different plant food materials during drying.* Journal of Food Engineering, 2015. **146**: p. 209-226. 10.1016/j.jfoodeng.2014.09.011